Charge independence, charge symmetry breaking in the *S*-wave nucleon-nucleon interaction, and renormalization

A. Calle Cordón,[1,*] M. Pavón Valderrama,[2,†] and E. Ruiz Arriola[3,‡]

[1]*Thomas Jefferson National Accelerator Facility, Newport News, Virginia 23606, USA*

[2]*Departamento de Física Teórica and Instituto de Física Corpuscular (IFIC), Centro Mixto CSIC–Universidad de Valencia, Institutos de Investigación de Paterna, Aptd. 22085, E-46071 Valencia, Spain*

[3]*Departamento de Física Atómica, Molecular y Nuclear and Instituto Carlos I de Fisica Teórica y Computacional, Universidad de Granada, E-18071 Granada, Spain*

(Received 2 June 2011; revised manuscript received 12 January 2012; published 22 February 2012)

We explore the interplay between renormalization, charge independence and charge symmetry breaking (CIB and CSB) in *S*-wave nucleon-nucleon scattering. The renormalizability requirement generates *universality functions*, that is, correlations between the low-energy scattering observables in the neutron-neutron, neutron-proton, and proton-proton systems. The universality functions only depend on the (known) form of the nucleon-nucleon potential at long distances and, in particular, they do not require any assumptions about short-range CIB and CSB effects. In addition, the inclusion of Coulomb effects is trivial for the particular case of proton-proton scattering, allowing us to relate strong and Coulomb scattering observables. Within this approach, and using a one-boson-exchange potential, the previous correlations are shown to be phenomenologically satisfied without the need to introduce further parameters.

DOI: 10.1103/PhysRevC.85.024002 PACS number(s): 21.30.Fe, 03.65.Nk, 11.10.Gh, 13.75.Cs

I. INTRODUCTION

The understanding of charge dependence of strong interactions has been a crucial issue in nuclear physics (for reviews see, e.g., [1–4]). In fact, the simplest place where this issue can be studied is in the nucleon-nucleon interaction. As is well known, isospin invariance is not an exact symmetry of strong interactions. As a consequence nuclear forces have a small, but net, charge-dependent component. By definition, *charge independence* means invariance under any rotation in isospin space. A violation of this symmetry is referred to as charge independence breaking (CIB) and it means in particular that, in the isovector ($T = 1$) state, the proton-proton ($T_3 = +1$), neutron-proton ($T_3 = 0$), or neutron-neutron ($T_3 = -1$) strong interactions are different. A particular case, known as charge symmetry breaking (CSB), only considers the difference between proton-proton (pp) and neutron-neutron (nn) interactions. Further corrections are expected when, in addition, Coulomb forces are added to the proton-proton system [$pp(c)$].

However, which is the length scale governing charge independence and charge symmetry breaking? Actually, CIB and CSB are important in *S*-wave nucleon-nucleon scattering, where the unnaturally large value of the scattering length in the $^1S_0$ partial wave[1] triggers a strong short-distance sensitivity. The result is the amplification of the effects related to variations in the short-range interaction, that is, precisely in the region where the nuclear potential, and hence the mechanisms behind CIB and CSB, may be less reliable. The current understanding is that CIB, and in particular CSB, are due to a mass difference between the up and down quarks and electromagnetic interactions. On the hadronic level and, in particular, in the meson exchange description of the nuclear forces (see. e.g., [5,6] for reviews on these models), major causes of CIB and CSB [2–4] are effects explicitly related to (i) electromagnetic effects (mainly Coulomb), (ii) mass splitting of the isovector π and ρ mesons and different coupling constants, (iii) mass splitting between the different Δ-isobar charge states, and (iv) unknown short-distance effects which are usually described by models. Traditionally, the difference between the charge and neutral pion masses is believed to account for a big contribution to CIB, while the difference between the masses of the neutron and the proton represents the most basic cause for CSB. In fact, pion mass differences have been shown to account for 80% of the np-pp scattering length difference [7]. Some recent phenomenological analyses consider the differences coming from nucleon mass splitting and kinematical effects [8–10] but do not extract nn properties. In Ref. [11] 2π-exchange contributions, $\pi\rho$ diagrams, and other multimeson exchanges, including the Δ isobar as an intermediate state, were considered to explain the empirical CSB value accurately. In a similar line, in Ref. [12] the empirical CIB value is explained in terms of 2π-exchange contributions with Δ excitations, while the 3π and 4π exchanges are found to generate a negligible effect. The difficulties arising in multimeson exchange diagrams, and in particular the energy dependence that they create, were avoided in the Bonn potential [5] by introducing two effective scalar-isoscalar σ mesons simulating $2\pi + \pi\rho$ exchanges. In the CD-Bonn potential [13], CSB was included at the simplest one-boson-exchange diagrams.

*cordon@jlab.org

†mpavon@ific.uv.es

‡earriola@ugr.es

[1]The large value is caused by the presence of a virtual state, that is, a pole in the second Riemann sheet in the negative-energy axis.

Many authors have also proposed ρ-ω mixing as a key ingredient to understand CSB [14,15]. In Ref. [14], ρ-ω mixing is identified as the major source of CSB, while proton and neutron mass differences are considered to produce a minor effect. However, it should be noted that such a calculation might be hampered by the fact that the $g_{\omega NN}$ coupling constant occurring in the CSB piece of the interaction is about 40% larger than expected value from SU(3) symmetry ($g_{\omega NN} = 3g_{\rho NN} \sim 9$) and also from the actual value taken for the CSB potential. Fixed-s dispersion relations [16] yielded $g_{\omega NN} = 5.7 \pm 2.0$ and Vector-Meson-Dominance (VMD) $\omega \to e^+e^-$ decays prefer $g_{\omega NN} \sim 10$. η-π^0 mixing has been shown to be of some relevance as well [17].

The high sensitivity to short-range mechanisms underlying CIB and CSB has been a major motivation to pursue experimental determinations of the neutron-neutron scattering length by indirect methods (for a review see, e.g., Ref. [18] and references therein). A recent measurement of the nn scattering length using the π-d capture reaction yields (see also [19] for a review) $a_{nn} = -18.69(4)$ fm when corrected for magnetic interactions. The CSB analysis of the reaction $dd \to \pi^0\alpha$ [20] uses also the large and SU(3)-violating $g_{\omega NN}$ constant. A recent effective field theory (EFT) analysis yields $a_{nn} = -22.9 \pm 4.1$ fm [21].

The purpose of the present work is to approach the problem from the renormalization point of view. We do not attempt a high-precision calculation; rather, our goal is to gather some insight onto how to relate different two-nucleon channels. In this regard, while we consider the long-distance potential between the nucleons to be known, we use physical low-energy parameters, such as the scattering length, to encode the unknown short-distance physics. An interesting aspect of renormalization in the context of the one-boson-exchange (OBE) model [22,23] is that we can employ the natural SU(3) value of $g_{\omega NN}$ without spoiling the phenomenological description of nucleon-nucleon scattering at low energies. However, a problematic feature of the OBE model is that it generates divergences in the physical observables, the scattering length in particular, when we try to correlate the np, nn, and pp systems. The solution we propose to this problem is a short-distance renormalization condition, featuring charge independence, which guarantees the finiteness of the correlations. As we will see, this renormalization condition works quite well on the phenomenological level. This approach differs from the traditional point of view, which we have briefly reviewed in the previous paragraphs, and from the EFT framework [24–29], in which the scattering lengths in the nn, np, and pp systems are simply assumed to be basically unrelated. In contrast, we pursue here the possible connection between the three two-nucleon isovector states from a new perspective which actually lies in between the traditional and the EFT approaches. In particular, we assume one of the scattering lengths to be known and then exploit the EFT concept of short-distance insensitivity[2] to determine all other scattering lengths and phase shifts from the requirement of finiteness of the scattering amplitude (that is, renormalizability).

The paper is organized as follows: in Sec. II we motivate the use of renormalization in the context of the NN interactions with or without Coulomb forces (see also Appendix A). This serves as preparatory material for the further developments in this work. In Sec. III we study CIB and CSB effects for np, nn, and pp (strong and Coulomb) systems, and we formulate *universality relations* which correlate the previously mentioned systems. In Sec. IV, by requiring finiteness, we propose a short-distance connection which allows us to correlate the np, nn, $pp(s)$, and $pp(c)$ scattering lengths. A further application of this approach, which we present in Appendix B, is the correlation of the Gamow-Teller matrix elements employed in np radiative capture and the pp fusion process. Finally, in Sec. V we present our conclusions.

II. STANDARD AND RENORMALIZATION APPROACHES

A. The OBE potential

In this section we briefly review the main ideas behind renormalization in coordinate space for the OBE potentials (for a more detailed account see, e.g., Ref. [22]) since they play a fundamental role in what follows. To provide a comprehensive perspective we compare it with the more traditional viewpoint of regulating the singular meson-exchange potentials. The crucial distinction lies in the sensitivity to short-distance details: from the renormalization point of view we expect complete insensitivity to these details. In contrast, a regularization procedure only guarantees the finiteness of the results. For definiteness, let us analyze as an illustrative example the phenomenologically successful $^1S_0$ OBE potential [5,13]

$$V(r) = -\frac{g_{\pi NN}^2 m_\pi^2}{16\pi M_N^2}\frac{e^{-m_\pi r}}{r} - \frac{g_{\sigma NN}^2}{4\pi}\frac{e^{-m_\sigma r}}{r} + \frac{g_{\omega NN}^2}{4\pi}\frac{e^{-m_\omega r}}{r} - \frac{f_{\rho NN}^2 m_\rho^2}{8\pi M_N^2}\frac{e^{-m_\rho r}}{r}, \quad (1)$$

where $g_{\sigma NN}$ is a scalar-type coupling, $g_{\pi NN}$ is a pseudo-scalar coupling, $g_{\omega NN}$ is a vector coupling, and $f_{\rho NN}$ is a tensor derivative coupling (see [5] for notation). We neglect for simplicity nucleon mass effects and a tiny η contribution. We take $m_\pi = 138$ MeV, $M_N = 939$ MeV, $m_\rho = 770$ MeV, $m_\omega = 783$ MeV and $g_{\pi NN} = 13.1$, which seem firmly established. The OBE potential, Eq. (1), corresponds to a long-distance expansion of the potential. On the other hand, NN scattering in the elastic region below the pion production threshold involves c.m. momenta $p < p_{\max} = 400$ MeV. Given the fact that $1/m_\omega = 0.25$ fm $\ll 1/p_{\max} = 0.5$ fm we expect heavier mesons to be irrelevant and ρ and ω themselves to be of marginal importance. This naive expectation is, however, not fulfilled in the traditional approach [5,13].

[2]From a renormalization point of view, by short-distance insensitivity we refer both to cutoff and regulator dependence. Clearly, when the cutoff is removed we expect regulator independence. However, we face the impossibility of checking *all* possible regulators, but still it is natural to expect that most of the regulator dependence is covered by fixing a regulator and varying the cutoff. This interpretation is the common practice within renormalization theory in quantum field theory.

TABLE I. Fits to the $^1S_0$ phase shift of the Nijmegen group [9] using the OBE potential with a charge-dependent OPE part. We take $m_{\pi^0} = 134.97$ MeV, $m_{\pi^+} = 139.57$ MeV, $g_A = 1.29$, and $f_\pi = 92.4$ MeV [31]. DOF stands for degrees of freedom. We neglect the CSB coming from the ρ meson and take $m_\rho = m_\omega = 770$ MeV fitting m_σ, $g_{\sigma NN}$, and $g^*_{\omega NN}$. We use the value $\alpha_{np} = -23.74$ MeV as an input (in boldface) when renormalizing.

BC	r_c (fm)	m_σ (MeV)	$g_{\sigma NN}$	$g^*_{\omega NN}$	χ^2/DOF	α_0 (fm)	r_0 (fm)
Regular solution I	0	498.2(7)	9.488(11)	7.94(2)	0.480	−23.737	2.678
Regular solution II	0	550.72(4)	13.87(13)	20.10(24)	0.674	−23.738	2.679
Renormalizing	0	490(17)	8.7(6)	0(5)	0.289	**−23.74**	2.672

In the following we will make the approximation $m_\rho = m_\omega$, especially when making fits of the coupling parameters to the $^1S_0$ phases. Under the previous approximation it is convenient to define

$$g^*_{\omega NN} = \sqrt{g^2_{\omega NN} - \frac{f^2_{\rho NN} m^2_\rho}{2M^2_N}} \tag{2}$$

in such a way that the combined ω-ρ potential reads

$$\frac{g^2_{\omega NN}}{4\pi}\frac{e^{-m_\omega r}}{r} - \frac{f^2_{\rho NN} m^2_\rho}{8\pi M^2_N}\frac{e^{-m_\rho r}}{r} \simeq \frac{(g^*_{\omega NN})^2}{4\pi}\frac{e^{-m_\omega r}}{r}. \tag{3}$$

The previous simplification is useful since it avoids correlations between $g_{\omega NN}$ and $f_{\rho NN}$ in the $^1S_0$ channel. For SU(3) values of $g_{\omega NN} \sim 9$ or VMD $\omega \to e^+e^-$ electromagnetic decays of $g_{\omega NN} \sim 10.5$ and typical ρ-tensor values $f_{\rho NN} \sim$ 14–18, one has $g^*_{\omega NN} \sim$ 0–7.

B. Standard approach

In the traditional approach [5,13] the problem is essentially handled by solving the reduced Schrödinger equation, which for the S-wave case reads

$$-u''_k(r) + M_N\, V(r) u_k(r) = k^2 u_k(r), \tag{4}$$

with $k = \sqrt{M_N E}$ the c.m. momentum, M_N the nucleon mass, and $V(r)$ the OBE potential of Eq. (1). The Schrödinger equation is a second-order differential equation and it has two linearly independent solutions. The physical solution is usually determined by the regularity condition at the origin, i.e.,

$$u_k(0) = 0. \tag{5}$$

This boundary condition for the Schrödinger equation implicitly assumes that we are taking the potential seriously all the way down to the origin.[3]

The asymptotic behavior of the reduced wave function for $r \gg 1/m_\pi$ is given by

$$u_k(r) \to \frac{\sin[kr + \delta_0(k)]}{\sin\delta_0(k)}, \tag{6}$$

where $\delta_0(k)$ is the S-wave phase shift. For the potential described by Eq. (1), the phase shift is an analytic function of k with branch cuts located at $k = \pm i m_\pi/2, \pm i m_\sigma/2$, etc. This means in particular that for momenta below the first branch cut, $|k| \leqslant m_\pi/2$, we can expand the phase shift by means of the effective range expansion [30]

$$k\, \cot\delta_0(k) = -\frac{1}{\alpha_0} + \frac{1}{2} r_0 k^2 + \sum_{n=2}^{\infty} v_n k^{2n}, \tag{7}$$

where α_0 is the scattering length, r_0 is the effective range, and the v_n are shape parameters.

In the traditional approach [5,13] *everything* is obtained from the potential, which is assumed to be valid for $0 \leqslant r < \infty$. In practice, strong form factors are included, mimicking the finite nucleon size and reducing the short-distance repulsion of the potential, but the regular boundary condition is always kept. One of the difficulties with this point of view has to do with the fact that the $^1S_0$ scattering length is unnaturally large, $\alpha_0 = -23.74(2)$ fm, while the effective range is natural, $r_0 = 2.77(4)$ fm (approximately twice the pion Compton wavelength, $\sim 2/m_\pi$). This has dramatic consequences regarding the short-distance sensitivity, as we will show below.

A fit to the np averaged data of Ref. [9] in the $^1S_0$ channel yields two possible solutions (see Table I).[4] Thus, we have two *good incompatible fits*. A remarkable aspect is the fact that the vector meson coupling constant is accurately well determined. Actually, if we assume that we have fitted the potential, Eq. (1), to reproduce α_0, a tiny change in the potential $V \to V + \Delta V$ has a dramatic effect on α_0, since one obtains

$$\Delta\alpha_0 = \alpha_0^2 M_N \int_0^\infty \Delta V(r) u_0(r)^2 dr, \tag{8}$$

a quadratic effect in a large α_0. As a result, potential parameters must be fine tuned, as can be deduced from the previous fits. Thus, despite the undeniable success in fitting the data, this sensitivity to short distances fixes in particular $g_{\omega NN}$ to high precision and actually to a very different value than expected from other sources. We identify this fine-tuning mechanism as the reason underlying the large $g_{\omega NN}$ coupling quoted in the OBE potential models (see, e.g., [5,13]).

However, it is worth mentioning that the two different scenarios correspond to selecting a potential possesing spurious bound states or not. The spurious-bound-state problem has

[3]Of course, in a more conventional setup, strong form factors accounting for the finite nucleon size should be included but they play a marginal role in the discussion of CSB.

[4]To keep the analysis as simple as possible we choose the average value of the Nijmegen potentials [9] which reproduce the Partial-Wave-Analysis (PWA) [8] with χ^2/DOF ~ 1 and take the corresponding standard deviation as an error estimate.

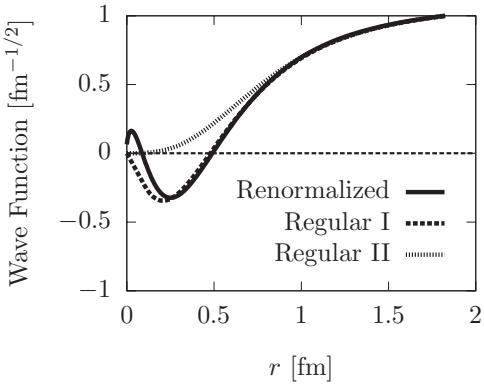

FIG. 1. Zero-energy wave function for the singlet np $^1S_0$ channel as a function of distance (in femtometers) and for the different scenarios with large and small ω couplings. This wave function goes asymptotically to $u_0(r) \to 1 - r/\alpha_0$, with $\alpha_0 = -23.74$ fm, the scattering length in this channel. The zero at about $r = 0.5$ fm signals the existence of a spurious bound state.

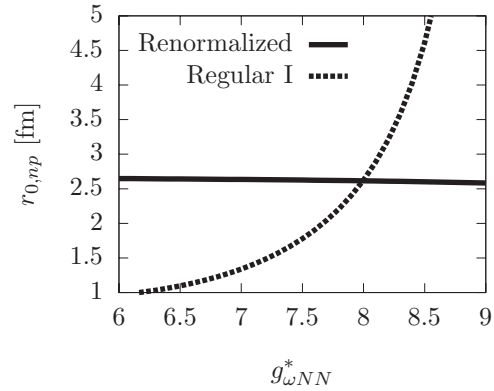

FIG. 2. Dependence of the effective range with respect to $g^*_{\omega NN}$ in the regular case with a small coupling constant and in the renormalized one.

been discussed in Ref. [22] at length; the number of inner zeros of the zero-energy wave function provides the number of bound states. For illustration we represent the zero-energy wave function in Fig 1. In the regular case, the OBE potential with a big $g^*_{\omega NN}$ is free of bound states. However, if a small $g^*_{\omega NN}$ is chosen, then one has to deal with a bound state which does not exist and it is hence spurious.[5]

C. Renormalization approach for finite-range interactions

The previous results do not comply with the intuitive expectation of insensitivity of low-energy physical observables with respect to the specific details of the potential in the short-distance region. Otherwise, where should one stop? This is the basic motivation of the renormalization viewpoint. The way to proceed is to impose renormalization conditions which eliminate the short-range sensitivity at the expense of treating low-energy parameters as independent variables from the potential. An example of a renormalization condition (RC) is to fix the scattering length, with the consequence of avoiding the fine-tuning problem summarized by Eq. (8). In other words, we trade the explicit dependence of the results on the short-range parameters of the potential for low-energy observables.

In principle there are several ways in which one can impose renormalization conditions (see, e.g., the discussion in Refs. [32,33]). Here we use the boundary conditions approach, which fits our needs perfectly. The idea is to substitute the regularity condition of the Schrödinger equation, $u_k(0) = 0$, by an arbitrary boundary condition at the origin:

$$L_k(0) = \frac{u'_k(0)}{u_k(0)}. \tag{9}$$

The regularity condition $u_k(0) = 0$ corresponds to taking the limit $L_k(0) \to \infty$; by changing the precise value and energy dependence of $L_k(0)$, the values of low-energy observables can be fixed. Here we will consider an energy-independent boundary condition, which ensures orthogonality of states. This restriction implies that there is only one free parameter. For example, if we want to fix the scattering length, we will solve the corresponding equation for the zero-energy wave function $u_0(r)$, with a suitable asymptotics,

$$-u''_0(r) + M_N\, V(r) u_0(r) = 0, \tag{10}$$

$$u_0(r) \to 1 - \frac{r}{\alpha_0}, \tag{11}$$

but, instead of solving the previous equation from $r = 0$ to $r \to \infty$, we solve it downward from infinity to the origin. Using the superposition principle one gets the following correlation between r_0 and α_0:

$$r_0 = A_0 + \frac{B_0}{\alpha_0} + \frac{C_0}{\alpha_0^2}, \tag{12}$$

where A_0, B_0, and C_0 are numbers depending only on the potential (see Ref. [22] for details). The interesting feature is that the dependence of the effective range with respect to short-range parameters of the potential is greatly diminished. The short-distance sensitivity can be vividly seen in Fig. 2, where the regular (parabolalike curve) and the renormalized (flat curve) effective range for the OBE potential are shown as a function of $g^*_{\omega NN}$. For simplicity, only the solution with small $g^*_{\omega NN}$ (Regular solution I) is represented.

The finite-energy solutions and the phase shifts can be obtained from an orthogonality condition [22], which after introducing a short-distance cutoff radius, r_c, implies

$$\lim_{r_c \to 0} \frac{u'_k(r_c)}{u_k(r_c)} = \lim_{r_c \to 0} \frac{u'_0(r_c)}{u_0(r_c)}, \tag{13}$$

providing the initial boundary conditions for the finite-energy Schrödinger equation, Eq. (4). We normalize the scattering wave function as follows:

$$u_k(r) \to \frac{\sin(kr + \delta_0)}{\sin \delta_0}. \tag{14}$$

[5]Note that regular solution II corresponds to a stronger short-distance repulsion than solution I. Thus in the classically forbidden region the wave function is accordingly much smaller in case II than in case I, as can be seen in Fig. 1.

If we use the superposition principle [22] and the orthogonality constraint, Eq. (13), the phase shift depends on the scattering length explicitly: $k \cot \delta_0$ is a bilinear mapping of α_0,

$$k \cot \delta_0 = \frac{\alpha_0 \mathcal{A}(k) + \mathcal{B}(k)}{\alpha_0 \mathcal{C}(k) + \mathcal{D}(k)}, \tag{15}$$

where the functions $\mathcal{A}$, $\mathcal{B}$, $\mathcal{C}$, and $\mathcal{D}$ are even functions of k which depend solely on the potential and not on the scattering length, α_0. Actually, by making a systematic expansion of the wave function as a power series of k, $u_k(r) = u_0(r) + k^2 u_2(r) + \ldots$ one may relate the effective range expansion in Eq. (7) and the corresponding low-energy threshold parameters. In particular, Eq. (12), is reproduced with a suitable identification of the functions $\mathcal{A}(k)$, $\mathcal{B}(k)$, $\mathcal{C}(k)$, and $\mathcal{D}(k)$.

Finally, we can use the previous procedure to fit the np averaged data of Ref. [9] in the $^1S_0$ channel (once we have fixed the scattering length to its experimental value), yielding the values in Table I. We can see the large uncertainty on the value of $g^*_{\omega NN}$, which shows that there is a greater insensitivity to shorter distances after renormalizing. This agrees with the previous remarks on the sensitivity of the effective range on $g^*_{\omega NN}$, illustrated in Fig. 2. Let us note further that, as discussed in Ref. [22], the renormalization scenario also has a spurious bound state as in the small-$g^*_{\omega NN}$ regular solution case (see Fig. 1). The current discussion would be modified by the inclusion of form factors which incorporate the finite nucleon size. However, because of the short-distance insensitivity, form factors turn out to play a marginal role [22] after renormalization.

D. Renormalization with Coulomb interactions

The extension of the previously discussed renormalization approach to the case of proton-proton scattering, where the infinite range of the Coulomb interaction plays a role, is straightforward. The corresponding S-wave reduced Schrödinger equation is

$$-u_k^{C\prime\prime} + M_p \left(V_{pp}(r) + \frac{\alpha}{r}\right) u_k^C = k^2 u_k^C, \tag{16}$$

where M_p is the proton mass, $V_{pp}(r)$ is the strong proton-proton potential, and $\alpha \simeq 1/137$ is the fine-structure constant. Actually, the discussion is tightly linked to the corresponding one for the two potential formula presented by two of us [35].

The definition of the phase shifts in the presence of the Coulomb potential is related to the behavior of the wave function at long distances, which is given by

$$u_k^C(r) \to \cot \delta_0^C(k) F_0(\eta, \rho) + G_0(\eta, \rho), \tag{17}$$

where $\delta_0^C(k)$ is the Coulomb-modified proton-proton phase shift and $F_0(\eta, \rho)$ and $G_0(\eta, \rho)$, with $\eta = 1/ka_B$ and $\rho = kr$, are the S-wave Coulomb wave functions [36]. The u_k^C wave function is the solution to the reduced Schrödinger equation, Eq. (16). The $F_0(\eta, \rho)$ and $G_0(\eta, \rho)$ wave functions behave asymptotically ($r \to \infty$) as

$$F_0 \to \sin(kr - \eta \log(2kr) + \sigma_0), \tag{18}$$

$$G_0 \to \cos(kr - \eta \log(2kr) + \sigma_0), \tag{19}$$

with σ_0 the Coulomb phase shift, which is defined as

$$e^{2i\sigma_0} = \frac{\Gamma(1 + i\eta)}{\Gamma(1 - i\eta)}. \tag{20}$$

The phase shift in the presence of the infinite-ranged Coulomb force does not obey the usual effective range expansion, which is valid for short-ranged potentials, but obeys a Coulomb-modified effective range expansion, given by

$$k \cot \delta_0^C C^2(\eta) + \frac{2}{a_B} h(\eta) = -\frac{1}{\alpha_{0,C}} + \frac{1}{2} r_{0,C} k^2 + \sum_{n=2}^{\infty} v_{n,C} k^{2n}, \tag{21}$$

with $C(\eta)$ and $h(\eta)$ defined as

$$C^2(\eta) = \frac{2\pi\eta}{e^{2\pi\eta} - 1}, \tag{22}$$

$$h(\eta) = \eta^2 \sum_{n=1}^{\infty} \frac{1}{n(n^2 + \eta^2)} - \log \eta - \gamma_E. \tag{23}$$

After some manipulations (see Appendix A for details) we obtain the following correlation between the Coulomb-modified hadronic scattering length and effective range:

$$r_{0,C} = A_0^C + \frac{B_0^C}{\alpha_{0,C}} + \frac{C_0^C}{\alpha_{0,C}^2}, \tag{24}$$

which is a direct generalization of Eq. (12) for the non-Coulomb case. Likewise, for the finite-energy case it is straightforward to obtain the correlation

$$k \cot \delta_0^C C^2(\eta) + \frac{2}{a_B} h(\eta) = \frac{\alpha_{0,C} \mathcal{A}^C(k) + \mathcal{B}^C(k)}{\alpha_{0,C} \mathcal{C}^C(k) + \mathcal{D}^C(k)}, \tag{25}$$

where $\mathcal{A}^C(k)$, $\mathcal{B}^C(k)$, $\mathcal{C}^C(k)$, and $\mathcal{D}^C(k)$ are analytic functions of the c.m. momentum and play a similar role as in Eq. (15).

E. Summary of the renormalization process

The renormalization procedure proposed in this section can be summarized as follows:

(i) For a given scattering length α_0, integrate in the zero-energy wave function $u_0(r)$ with Eq. (10) down to the cutoff radius r_c. This is the renormalization condition.
(ii) Implement orthogonality at the cutoff radius through the boundary condition as in Eq. (13).
(iii) Integrate out the finite-energy wave function $u_k(r)$ with Eq. (4) and determine the phase shift $\delta_0(p)$ from Eq. (6).
(iv) Remove the cutoff (take the limit $r_c \to 0$) to assure model (regulator) independence.

This allows us to compute δ_0 (and hence r_0, v_2) from (i) the potential $V(r)$ and (ii) the scattering length α_0 as independent information. Of course, this also applies to the Coulomb case with suitable modifications. Note that this is equivalent to considering, in addition to the regular solution, the irregular one. In momentum space this can be shown to be equivalent to introducing one counterterm in the cutoff Lippmann-Schwinger equation (see Ref. [33] for a

detailed discussion). Both Eq. (12) and Eq. (15) highlight this decorrelation between the potential and the scattering length. Contrary to common wisdom, but according to our intuitive expectations, no strong short-range repulsion is essential. The moral is that building α_0 *from* the potential is equivalent to absolute knowledge at short distances; as in the $^1S_0$ channel a strong fine tuning is at work. This example illustrates our point that the renormalization viewpoint tells us to what extent short-distance physics may be less well determined than is assumed in the traditional approach. This leads to a new perspective [22] to the phenomenology of OBE potentials without a need for a strong ω repulsion.

III. CHARGE SYMMETRY BREAKING

In the previous sections we have shown how the renormalization of the $^1S_0$ two-nucleon system can be carried out. This procedure allows us to determine the $^1S_0$ phase shifts for np, nn, pp, and $pp(c)$ from their corresponding scattering lengths α_{np}, α_{nn}, α_{pp}, and α^C_{pp}, respectively. The previous computation can be compared with the experimental values for these quantities in order to test the renormalization procedure.

Admitted values of the scattering lengths are [2–4],

$$\begin{aligned} \alpha^C_{0,pp} &= -7.8149(29)\ \text{fm}, \quad \alpha_{0,pp} = -17.3(4)\ \text{fm}, \\ \alpha_{0,nn} &= -18.8(3)\ \text{fm}, \quad \alpha_{0,np} = -23.77(9)\ \text{fm}, \end{aligned} \tag{26}$$

giving $\Delta\alpha_{\text{CIB}} \equiv (\alpha_{0,pp} + \alpha_{0,nn})/2 - \alpha_{0,np} = 5.7(3)$ fm and $\Delta\alpha_{\text{CSB}} \equiv \alpha_{0,pp} - \alpha_{0,nn} = 1.5(5)$ fm. For the effective range we have [2–4]

$$\begin{aligned} r^C_{pp} &= 2.769(14)\ \text{fm}, \quad r_{pp} = 2.85(4)\ \text{fm}, \\ r_{nn} &= 2.75(11)\ \text{fm}, \quad r_{np} = 2.75(5)\ \text{fm}, \end{aligned} \tag{27}$$

with $\Delta r_{0,\text{CIB}} = 0.05(8)$ fm and $\Delta r_{0,\text{CSB}} = 0.1(1)$ fm. As can be seen, the CIB and CSB are much larger for the scattering length than for the effective range. This can be partially explained by the unnaturally large value of the NN scattering length.

Before going further it is interesting to mention that the strong pp scattering observables are largely model-dependent quantities. This was unveiled by Sauer long ago [34] by carrying out a unitary short-range transformation, which, while keeping the Coulomb interaction scattering observables unchanged, allowed one to get almost any possible value for the corresponding pp strong counterpart. This issue has been also confirmed within the EFT approach [26] due to the onset of logarithmic divergences (see also [35]). In Sec. IV we will suggest a way to handle this difficulty.

To take into account the various physical effects which generate charge symmetry breaking, we consider the neutron-proton mass difference and the OPE *reduced* potentials, $U(r) = 2\mu V(r)$, defined as

$$\begin{aligned} U^{1\pi}_{pp}(r) &= -M_p\, f_\pi^2 \left(\frac{m_{\pi^0}}{m_{\pi^+}}\right)^2 \frac{e^{-m_{\pi_0} r}}{r}, \\ U^{1\pi}_{np}(r) &= -M_{np}\, f_\pi^2 \left[2\,\frac{e^{-m_{\pi_+} r}}{r} - \left(\frac{m_{\pi^0}}{m_{\pi^+}}\right)^2 \frac{e^{-m_{\pi_0} r}}{r}\right], \\ U^{1\pi}_{nn}(r) &= -M_n\, f_\pi^2 \left(\frac{m_{\pi^0}}{m_{\pi^+}}\right)^2 \frac{e^{-m_{\pi_0} r}}{r}, \end{aligned} \tag{28}$$

with $m_{\pi_0} = 134.97$ MeV and $m_{\pi_+} = 139.57$ MeV. M_n is the neutron mass and M_{np} is twice the reduced np mass, $2\mu_{np} = 2M_pM_n/(M_p + M_n)$. Therefore, for the OBE NN potential we have

$$\begin{aligned} V_{np}(r) &= V^{1\pi}_{np}(r) + V^{1\sigma}(r) + V^{1\rho}_{np}(r) + V^{1\omega}(r) + \cdots, \\ V_{nn}(r) &= V^{1\pi}_{nn}(r) + V^{1\sigma}(r) + V^{1\rho}_{nn}(r) + V^{1\omega}(r) + \cdots, \\ V_{pp}(r) &= V^{1\pi}_{pp}(r) + V^{1\sigma}(r) + V^{1\rho}_{pp}(r) + V^{1\omega}(r) + \cdots. \end{aligned} \tag{29}$$

Clearly, the potentials in the different channels are not very different from one to another quantitatively. Actually, the σ- and ω-exchange contributions coincide identically. On the other hand, the π and ρ take into account the different charged mesons which are exchanged. Obviously, one expects the symmetry breaking effects coming from π exchange to be more important than those from ρ exchange. Theoretical computations seem to support the previous result, giving $\Delta\alpha_{\text{CIB},\pi} = 3.24$ fm and $\Delta\alpha_{\text{CIB},\rho} = -0.29$ fm (see Ref. [12]). As a consequence, ρ mass differences are negligible.

The long-distance correlation between the scattering length and effective range looks like

$$r_{0,np} = A_{np} + \frac{B_{np}}{\alpha_{0,np}} + \frac{C_{np}}{\alpha^2_{0,np}}, \tag{30}$$

$$r_{0,pp} = A_{pp} + \frac{B_{pp}}{\alpha_{0,pp}} + \frac{C_{pp}}{\alpha^2_{0,pp}}, \tag{31}$$

$$r_{0,nn} = A_{nn} + \frac{B_{nn}}{\alpha_{0,nn}} + \frac{C_{nn}}{\alpha^2_{0,nn}}, \tag{32}$$

$$r^C_{0,pp} = A^C_{pp} + \frac{B^C_{pp}}{\alpha_{0,C,pp}} + \frac{C^C_{pp}}{\alpha^2_{0,C,pp}}, \tag{33}$$

while the phase shifts are given by

$$k\cot\delta_{0,np} = \frac{\alpha_{0,np}\mathcal{A}_{np}(k) + \mathcal{B}_{np}(k)}{\alpha_{0,np}\mathcal{C}_{np}(k) + \mathcal{D}_{np}(k)}, \tag{34}$$

$$k\cot\delta_{0,nn} = \frac{\alpha_{0,nn}\mathcal{A}_{nn}(k) + \mathcal{B}_{nn}(k)}{\alpha_{0,nn}\mathcal{C}_{nn}(k) + \mathcal{D}_{nn}(k)}, \tag{35}$$

$$k\cot\delta_{0,pp} = \frac{\alpha_{0,pp}\mathcal{A}_{pp}(k) + \mathcal{B}_{pp}(k)}{\alpha_{0,pp}\mathcal{C}_{pp}(k) + \mathcal{D}_{pp}(k)}, \tag{36}$$

$$C^2(\eta)\,k\,\cot\delta^C_{0,pp} + \frac{2}{a_B}\,h(\eta) = \frac{\alpha^C_{0,pp}\mathcal{A}^C_{pp}(k) + \mathcal{B}^C_{pp}(k)}{\alpha^C_{0,pp}\mathcal{C}^C_{pp}(k) + \mathcal{D}^C_{pp}(k)}. \tag{37}$$

We remind the reader that in these formulas the scattering lengths are independent of the potentials.

In Fig. 3 we show the universal functions $\mathcal{A}$, $\mathcal{B}$, $\mathcal{C}$, and $\mathcal{D}$ for the four cases considered. As can be seen, for nn, np, and pp and in the range of relevant momenta $p \leqslant 400$ MeV they turn out to practically coincide numerically as a consequence of the similarity of the corresponding potentials. This means in particular that most of the CIB and CSB effects for $p \leqslant 400$ MeV come solely from the difference in the scattering length (since there are no genuine sizable effective range effects). It is also interesting to see that the Coulomb

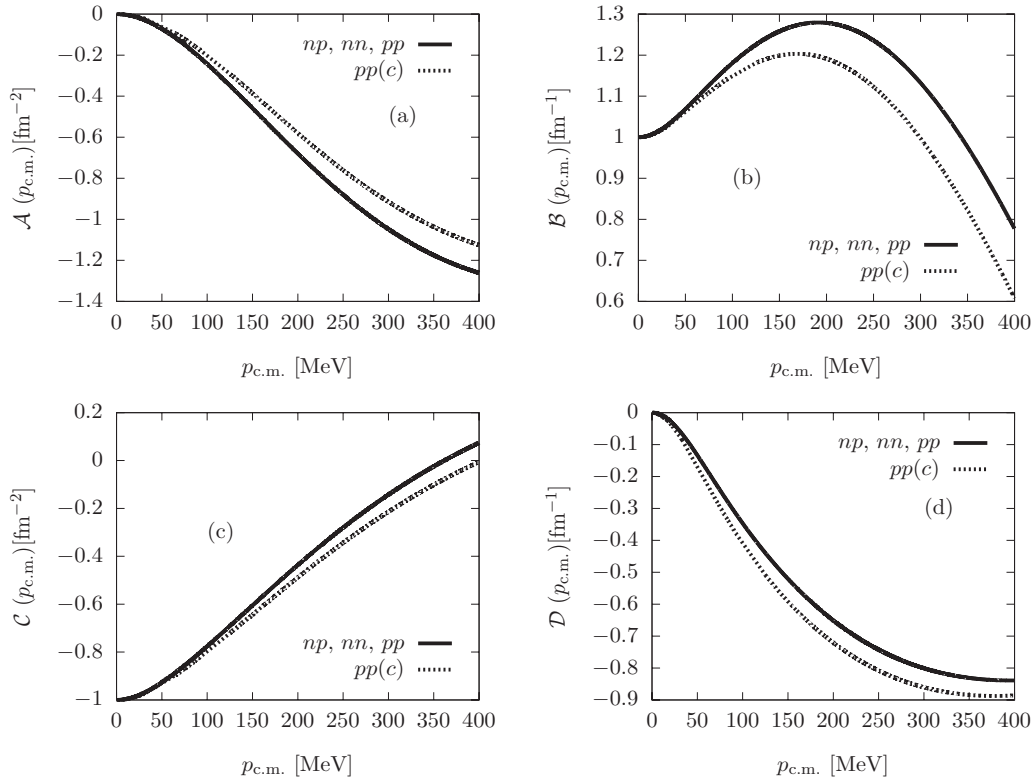

FIG. 3. The universal functions $\mathcal{A}$, $\mathcal{B}$, $\mathcal{C}$, and $\mathcal{D}$ defined by Eqs. (34)–(37) and Eq. (A4) in appropriate length units as a function of the c.m. momentum p (in MeV) for the four ${}^1S_0$ channels np, pp, nn, and $pp(c)$. These functions depend on the potentials $V_{np}(r)$, $V_{nn}(r)$, $V_{pp}(r)$, and $V^C_{pp}(r)$ only but are independent of the scattering lengths.

corrections to the $pp(c)$ universal functions differ increasingly for higher energies.

IV. THE SHORT-DISTANCE CONNECTION

As is well known, at large energies the np and $pp(c)$ phase shifts resemble each other more closely than at low energies,[6] suggesting that charge invariance works better at short distances. Most of the charge invariance and charge symmetry breaking effects only influence the low-energy behavior, specifically the scattering lengths as given below Eq. (26). When one considers the effective range, the symmetry breaking effects are already one-tenth that in the scattering length case, being of the order of a tenth of a fermi. The problem is how to explain these differences.

In what follows we argue how this could be done without going into all the details and intricacies of the NN interaction precisely in the short-distance region where our lack of knowledge is magnified due to the unnaturally large scattering length. In the traditional approach all the CIB and CSB effects are explained via the OBE potential, Eq. (1). The Schrödinger equation is integrated from the origin to infinity with regular boundary conditions and all the differences between scattering observables must come from the potential. In the renormalization approach things get more involved: there are explicit contributions coming from short-distance operators which are used to weaken the short-distance sensitivity. The problem is how to implement either charge independence or its breaking within this approach in a regulator-independent way. If we assume that at lowest order all the charge-independence breaking comes from the finite-range potential, one is tempted to identify short-distance charge independence with identical logarithmic boundary conditions. For example, if we relate the nn and np problems with

$$\frac{u'_{nn}(r_c)}{u_{nn}(r_c)} = \frac{u'_{np}(r_c)}{u_{np}(r_c)}, \tag{38}$$

we will find that this relation produces log-divergent results for any Yukawa potential in the limit $r_c \to 0$. Another option is to regulate with a short-distance delta potential

$$V_C(r; r_c) = \frac{C_0(r_c)}{4\pi r_c^2}\,\delta(r - r_c), \tag{39}$$

which corresponds to a specific regularization of the δ function potential, and assume that charge independence at short distance is equivalent to $C_{0,nn}(r_c) = C_{0,np}(r_c) = C_{0,pp}(r_c) = C_0(r_c)$. This choice leads to the following logarithmic

[6]In the presence of Coulomb forces there is an additional effective screening at larger momenta; for a maximum c.m. momentum, i.e., a de Broglie wavelength of 0.5 fm, such a screening induces a difference of about 1°.

boundary condition between nn and np:

$$\frac{1}{M_n}\left(\frac{u'_{nn}(r_c)}{u_{nn}(r_c)}-\frac{1}{r_c}\right)=\frac{1}{M_{np}}\left(\frac{u'_{np}(r_c)}{u_{np}(r_c)}-\frac{1}{r_c}\right). \quad (40)$$

The counterterm conditions also run into the same cutof-dependence problems as the logarithmic boundary condition. This means in particular that the two previous proposals are regulator dependent, and hence model dependent, and pose a serious problem on what is meant by charge independence of short-distance operators. We will show that, by using the hypothesis of charge independence at short distances together with finiteness, a relation between them can be established which works rather satisfactorily at both a mathematical as well as a phenomenological level.

At short distances all the pp (strong and Coulomb), np, and nn potentials have an attractive Coulomb-like behavior

$$2\mu_{NN}\,V_{NN}(r)\xrightarrow[r\to 0]{}-\frac{1}{R\,r}, \quad (41)$$

where NN either refers to pp (strong), pp (Coulomb), np, or nn, and μ_{NN} and V_{NN} are the corresponding reduced mass and potential. The constant R depends on the problem; for the OBE potential of Eq. (1) with the additional simplification of taking $m_\omega = m_\rho$ and defining $g^*_{\omega NN}$, we get the scales

$$\frac{1}{R_{np}}=M_{np}\left(f^2_{\pi NN}+g^2_{\sigma NN}-{g^*_{\omega NN}}^2\right), \quad (42)$$

$$\frac{1}{R_{nn}}=M_{n}\left(f^2_{\pi NN}+g^2_{\sigma NN}-{g^*_{\omega NN}}^2\right), \quad (43)$$

$$\frac{1}{R_{pp}}=M_{p}\left(f^2_{\pi NN}+g^2_{\sigma NN}-{g^*_{\omega NN}}^2\right), \quad (44)$$

$$\frac{1}{R^C_{pp}}=M_{p}\left(f^2_{\pi NN}+g^2_{\sigma NN}-{g^*_{\omega NN}}^2-\alpha\right). \quad (45)$$

As a consequence of the short-distance Coulomb singularity, the wave function at short distances approximately behaves as linear combinations of *attractive* Coulomb wave functions

$$u_{k,NN}(r)\to a\,\frac{R}{2}\sqrt{x}\,J_1(2\sqrt{x})+b\,2\sqrt{x}\,Y_1(2\sqrt{x}) + O(mr, mR, k^2r^2, r/R), \quad (46)$$

where J_1 and Y_1 are Bessel functions. The constants a and b determine the correct linear combination, R can be R_{nn}, R_{np}, or R_{pp} (strong and Coulomb), $x = 2r/R$, and m generically denotes the mass of any of the exchanged bosons. The expected mR contributions will only shift the irregular solutions by a constant.

The previous behavior can be quite problematic as we can see if we consider the log derivative of the wave function at small enough cutoff radii, which behaves as

$$R\,\frac{u'_{k,NN}(r_c)}{u_{k,NN}(r_c)}\to -2\gamma_E-\frac{\pi}{4}\,R\,\lambda-\log\frac{r_c}{R}+\ldots, \quad (47)$$

where $\gamma_E = 0.57722$ is the Euler-Mascheroni constant, $\lambda = a/b$, and the dots refer to higher order terms, like mr_c or $k^2r_c^2$ corrections. With this behavior, we can see that naively identifying the log derivative at the cutoff radius in order to obtain correlations between observables of the different two-nucleon systems will yield divergent results. For example, relating np and nn,

$$\frac{u'_{k,nn}(r_c)}{u_{k,nn}(r_c)}=\frac{u'_{k,np}(r_c)}{u_{k,np}(r_c)}, \quad (48)$$

generates the singularity

$$\frac{1}{R_{np}}\log\left(\frac{r_c}{R_{np}}\right)-\frac{1}{R_{nn}}\log\left(\frac{r_c}{R_{nn}}\right). \quad (49)$$

This singularity is indeed mild, as it can only be seen at very short distances (depending on how small the difference is between $1/R_{nn}$ and $1/R_{np}$), but sooner or later the irregular Coulomb solution will ruin our results.

Under these circumstances there is a quantity that can be constructed from the log derivative at short distance that is finite in the $r_c\to 0$ limit. This quantity is the following:

$$\mathcal{S}=R\,\frac{u'(r_c)}{u(r_c)}+\log\left(\frac{r_c}{R}\right),\quad r_c\ll R, \quad (50)$$

which is cutoff and energy independent. This suggests that different scattering problems, having different short-distance constants but the same logarithmic-scale dependence, can be connected in such a way that the scale dependence is eliminated. This is done by equating the corresponding $\mathcal{S}$'s,

$$\mathcal{S}_1=\mathcal{S}_2, \quad (51)$$

where 1 and 2 refer to two different $NN = nn, np, pp, pp(c)$, cases.[7]

We can give here two examples of the adequacy of the short-distance connection. The first one is to obtain the strong pp scattering length from the experimental Coulomb one, $\alpha^C_{0,pp}=-7.8149$ fm yielding $\alpha_{0,pp}=-18.46$ fm, a not unreasonable result [to be compared with the extraction $\alpha_{0,pp}=-17.3$ fm; see values in Eq. (26), where the error comes from model dependence]. The CD-Bonn potential gives a value of $\alpha_{0,pp}=-17.46$ fm. The extracted effective ranges are $r^C_{0,pp}=2.735$ fm and $r_{0,pp}=2.789$ fm. As a second example, by taking the np scattering length as input, $\alpha_{0,np}=-23.74$ fm, we can obtain all the NN low-energy parameters (LEP), giving $\alpha_{0,nn}=-19.626$ fm, $\alpha_{0,pp}=-17.806$ fm, and $\alpha^C_{0,pp}=-7.706$ fm for the scattering lengths and $r_{0,np}=2.672$ fm, $r_{0,nn}=2.771$ fm, $r_{0,pp}=2.802$ fm, and $r^C_{0,pp}=2.747$ fm for the effective ranges. A remarkable aspect of the previous computation is that one obtains $\Delta\alpha_{\rm CIB}=5.024$ fm, $\Delta r_{\rm CIB}=0.115$ fm, $\Delta\alpha_{\rm CSB}=1.82$ fm, and $\Delta r_{\rm CSB}=0.031$ fm, which agree within error estimations with the expected values for these quantities [2–4]. In Table II we summarize the results obtained with the short-distance connection (renormalized) and the one obtained by integrating upward with a regular

[7]Note that the result in the scattering lengths due to say two potentials such as the Coulomb potential, V_C, and the hadronic (strong) potential, V_{pp}, is not additive; namely, $\alpha^C_{0,pp}\neq\alpha_{0,pp}+\Delta\alpha^C_0$, where $\Delta\alpha^C_0$ would be the first-order correction due to the Coulomb potential. This is because perturbation theory is not applicable to either of the two potentials, even if distorted waves are used (see also Ref. [35]).

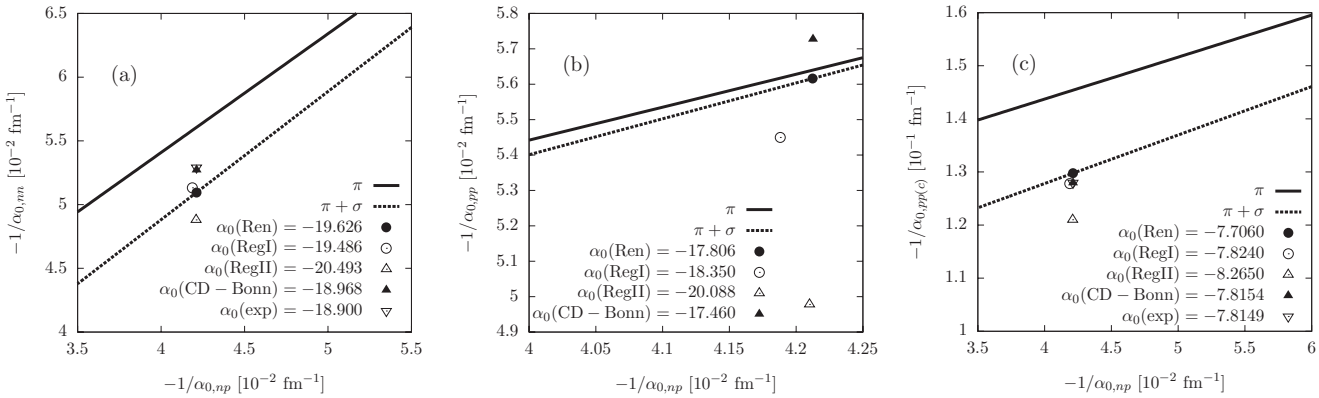

FIG. 4. The relationships between the *predicted* scattering lengths in the $^1S_0$ channel for nn, pp, and $pp(c)$ as a function of $\alpha_{0,np}$ when the successive π and $\pi+\sigma$ contributions are included. We plot inverse scattering lengths. Note the small scale.

boundary condition (regular). We can see that in the case of a big $g^*_{\omega NN}$ the regular solution does a poor job in calculating the LEP in other channels. The CD-Bonn potential [13] corresponds with this scenario, i.e., a big SU(3) breaking coupling constant but with no spurious bound state. Looking at this table one can understand why in this model a different mass for a fictitious σ meson is used in each NN channel. The strong fine tuning that appears in this situation hinders the relations between different NN problems.

An important ingredient in obtaining such a large change in the scattering length, and in particular large CIB, has to do with the fine tuning of the interactions; indeed the changes both in the (reduced) potential and in the zero-energy wave function are small. However, since the scattering length is large these tiny changes make dramatic differences in the scattering length. Recall that α_0 corresponds to the crossing of the asymptotic wave function with the x axis; thus a small change in a rather flat curve moves this crossing quite substantially. Thus, if we consider the $pp(s)$ channel versus the nn channel, which correspond to the same potential but different masses, we produce a big change in the scattering lengths [see, e.g., Eq. (8) with $M_N\,\Delta V \to \Delta M\,V(r)$ with $\Delta M = M_p - M_n$]. However, note that this big change does not occur for the effective ranges (see Table II).

A further interesting example of the adequacy of the short-distance connection is illustrated in Appendix B, where the Gamow-Teller matrix element appearing in the proton-proton fusion process is analyzed.

As can be seen from Table II the results depend on the chosen starting condition, illustrating the limitations of this short-distance connection. However, we have checked that the CSB and CIB effects agree within error with expected estimations in all cases. Moreover, note that the previous choice, Eq. (51), is not the only possible *covariant* short-distance connection, as we could have defined

$$\mathcal{S}' = R\,\frac{u'(r_c)}{u(r_c)} + \log\left(\frac{\lambda\, r_c}{R}\right), \qquad r_c \ll R, \tag{52}$$

with λ some arbitrary constant, which depends on the specific NN problem being considered. A natural choice is to take λ of order unity, which does not lead to much difference between different choices of $\mathcal{S}$ due to the weak logarithmic behavior. It must be stressed though that the results are not unique: arbitrary λ's can be introduced to better connect the different two-nucleon systems. As the hypothesis of the charge dependence of short-distance operators cannot be implemented in a completely model-independent way, we will chose to take $\lambda_{nn} = \lambda_{np} = \lambda_{pp}$ at first order. We have already seen that this simple condition generates quite accurate results, meaning that corrections due to the naive estimate $\lambda = 1$ are indeed small.

To clarify the implications of the short-distance connection, let us consider two different problems A and B, which have associated Coulomb length scales R_A and R_B. In other words, we have the differential equations

$$-u''_{k,A} + 2\mu_A\,V_A(r)u_{k,A}(r) = k^2 u_{k,A}(r), \tag{53}$$

$$-u''_{k,B} + 2\mu_B\,V_B(r)u_{k,B}(r) = k^2 u_{k,B}(r), \tag{54}$$

where the reduced potentials behave as $1/r$ at short distances:

$$2\mu_A\,V_A(r) \to -\frac{1}{R_A\,r}, \tag{55}$$

$$2\mu_B\,V_B(r) \to -\frac{1}{R_B\,r}. \tag{56}$$

These two problems are related at short distances through the boundary condition corresponding to the short-distance connection $\mathcal{S}_A = \mathcal{S}_B$:

$$R_B\,\frac{u'_{k,B}(r_c)}{u_{k,B}(r_c)} = \log\frac{R_A}{R_B} + R_A\frac{u'_{k,A}(r_c)}{u_{k,A}(r_c)}. \tag{57}$$

If we have only fixed the scattering length, the above condition becomes energy independent when the cutoff is small enough, which means that it can be evaluated with the zero-energy wave functions of the two-body systems A and B. By using the superposition principle, the previous zero-energy wave functions can be written as

$$u_{0,A}(r) = v_{0,A}(r) - \frac{1}{\alpha_A}w_{0,A}(r), \tag{58}$$

$$u_{0,B}(r) = v_{0,B}(r) - \frac{1}{\alpha_B}w_{0,B}(r). \tag{59}$$

TABLE II. NN low-energy parameters in the different scenarios. Renormalization only needs one scattering length (in bold face), np, $pp(c)$, or nn, as an input parameter, respectively. All the other parameters are calculated without ambiguities. Quoted errors reflect the input uncertainty in the scattering length only. The OBE potential parameters have been fitted in the np case and kept the same in the other cases. Here (c) means the Coulomb interaction is switched on.

NN	LEP	Ren. (np) ($g^*_{\omega NN} \sim 0$)	Ren. [$pp(c)$] ($g^*_{\omega NN} \sim 0$)	Ren. (nn) ($g^*_{\omega NN} \sim 0$)	Reg. I ($g^*_{\omega NN} \sim 8$)	Reg. II ($g^*_{\omega NN} \sim 20$)	CD-Bonn [13]	Exp. [13]
np	α_0 [fm]	**−23.74(2)**	− 24.91(3)	− 22.7(6)	− 23.737	− 23.738	− 23.738	− 23.74(2)
	r_0 [fm]	2.6716(2)	2.6602(3)	2.683(6)	2.678	2.677	2.671	2.77(5)
pp	α_0 [fm]	− 17.806(11)	− 18.46(2)	− 17.2(3)	− 18.350	− 20.088	− 17.46	–
	r_0 [fm]	2.8022(2)	2.7895(3)	2.815(7)	2.799	2.768	2.845	–
$pp(c)$	α_0 [fm]	− 7.706(2)	**−7.815(3)**	− 7.60(6)	− 7.824	− 8.265	− 7.8154	− 7.8149(29)
	r_0 [fm]	2.7470(2)	2.7348(3)	2.759(7)	2.641	2.693	2.773	2.769(14)
nn	α_0 [fm]	− 19.626(14)	− 20.42(2)	**−18.9(4)**	− 19.486	− 20.493	− 18.968	− 18.9(4)
	r_0 [fm]	2.7709(2)	2.7585(3)	2.783(7)	2.780	2.763	2.819	2.75(11)

These wave functions can be included in Eq. (57), yielding the following relation between the scattering lengths α_A and α_B of the two different problems:

$$\frac{a}{\alpha_A} = \frac{b}{\alpha_B} + c + \frac{d}{\alpha_A\,\alpha_B}. \tag{60}$$

Therefore, if we make the hypothesis of charge independence at short distances,

$$\mathcal{S}_{np} = \mathcal{S}_{nn} = \mathcal{S}_{pp} = \mathcal{S}^C_{pp}, \tag{61}$$

and use the superposition principle, we can write

$$u_{0,np}(r) = v_{0,np}(r) - \frac{1}{\alpha_{0,np}} w_{0,np}(r), \tag{62}$$

$$u_{0,nn}(r) = v_{0,nn}(r) - \frac{1}{\alpha_{0,nn}} w_{0,nn}(r), \tag{63}$$

$$u_{0,pp}(r) = v_{0,pp}(r) - \frac{1}{\alpha_{0,pp}} w_{0,pp}(r), \tag{64}$$

$$u^C_{0,pp}(r) = v^C_{0,pp}(r) - \frac{1}{\alpha^C_{0,pp}} w^C_{0,pp}(r), \tag{65}$$

so we get bilinear relations between all scattering lengths:

$$\frac{a_{nn}}{\alpha_{nn}} = \frac{b_{nn}}{\alpha_{np}} + c_{nn} + \frac{d_{nn}}{\alpha_{nn}\,\alpha_{np}}, \tag{66}$$

$$\frac{a_{pp}}{\alpha_{pp}} = \frac{b_{pp}}{\alpha_{np}} + c_{pp} + \frac{d_{pp}}{\alpha_{pp}\,\alpha_{np}}, \tag{67}$$

$$\frac{a^C_{pp}}{\alpha^C_{pp}} = \frac{b^C_{pp}}{\alpha_{np}} + c^C_{pp} + \frac{d^C_{pp}}{\alpha^C_{pp}\,\alpha_{np}}, \tag{68}$$

etc. In Fig. 4 we show the dependence of the scattering lengths as obtained from the np scattering length and the previous correlations. As can be seen, the correlations work rather well, confirming the idea that finiteness is a good criterion to implement charge independence of short-distance operators. Numerical values are listed in Table II when the experimental value of $\alpha_{0,np}$ is taken. Generally, one might expect $\mathcal{S}^C_{pp} = \mathcal{S}^S_{pp} + \alpha\mathcal{S}^{(1)}_{pp} + \ldots$. Our results are consistent with the expected smallness of the corrections.

We address now the interesting issue of how the errors in the fitting procedure to the np potentials propagate to the values of scattering lengths and effective ranges in the remaining

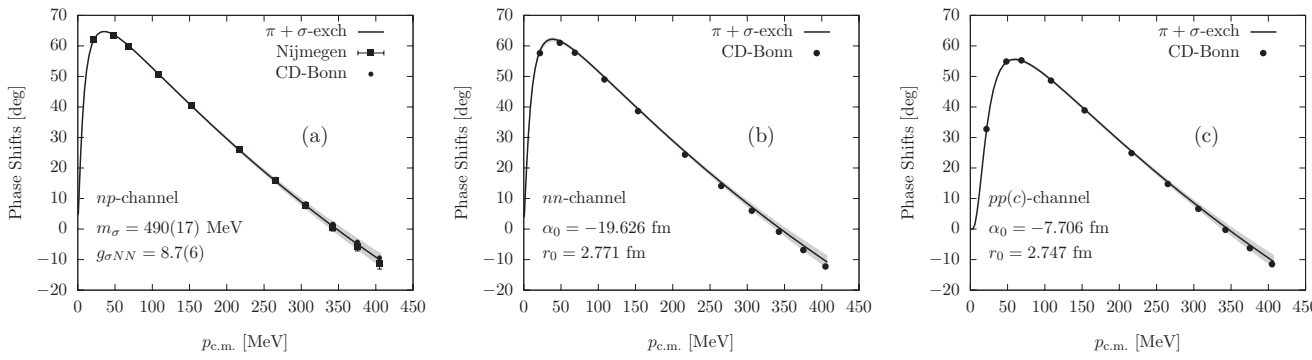

FIG. 5. Renormalized phase shifts for the OBE potential with CSB OPE + σ as a function of the c.m. momentum in the singlet $^1S_0$ channel. In panel (a) we show the fitted np phase shift to the Nijmegen results [9]. In panels (b) and (c) the *predicted* $pp(c)$ and nn are shown and compared to the CD-Bonn result [13], respectively. The band reflects the errors obtained from propagating the np fit parameters.

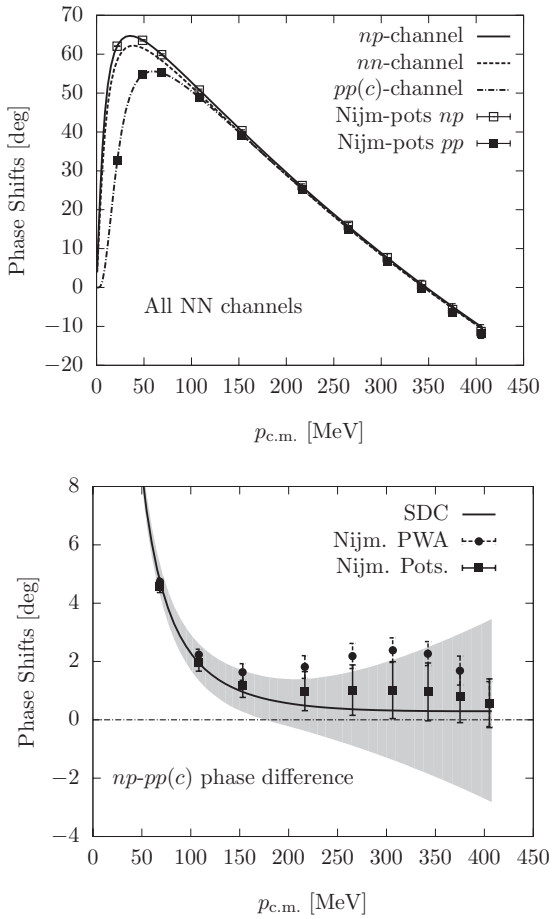

FIG. 6. Renormalized phase shifts for the OBE potential with CSB OPE + σ as a function of the c.m. momentum in the singlet $^1S_0$ channel. Upper panel: The fitted np phase shift to the Nijmegen potentials results as well as the *predicted* $pp(c)$ and nn compared to the Nijmegen potentials results for np and $pp(c)$ [8,9]. Lower panel: The predicted difference between np and $pp(c)$ phases (SDC) compared to the Nijmegen PWA and potential results [8,9]. In both cases the band and the error bars correspond to adding errors of np and $pp(c)$ in quadrature.

channels through the short-distance connection.[8] We obtain $\alpha_{0,nn} = -19.5(8)$ fm, $\alpha_{0,pp} = -17.8(3)$ fm, and $\alpha^C_{0,pp} = -7.7(1)$ fm for the scattering lengths and $r_{0,np} = 2.67(3)$ fm, $r_{0,nn} = 2.77(4)$ fm, $r_{0,pp} = 2.80(3)$ fm, and $r^C_{0,pp} = 2.75(4)$ fm for the effective ranges. This shows that, while we agree with experimental or recommended values [see Eqs. (26) and (27)], our uncertainties are rather reasonable, taking into account the simplicity of the approach. In fact, these error estimates comply with the variations obtained by varying the short-distance cutoff r_c below 0.4 fm.

It is interesting to see how the short-distance connection works at finite energy and, in particular, if a given specific NN channel is able to predict the phase shifts for the remaining channels. In Fig. 5 we plot the extracted nn and $pp(c)$ phase shifts when the OBE parameters have been fixed from the $^1S_0$ Nijmegen np phase shifts. We have computed these phase shifts by renormalizing in the np channel, i.e., by fixing $\alpha_{0,np}$ as input and integrating inward the Schrödinger equation, and then using Eq. (61) we connect with the other channels. The comparison with CD-Bonn estimates is satisfactory. Note that the only explicit CSB effect we include when comparing nn and $pp(s)$ is just the baryon mass difference. We include also our estimate of errors induced from the fit to np data, similarly to what was done above for the low-energy-threshold parameters. As a check we reproduce the errors from the fit in the np case.[9] In Fig. 6 we undertake a similar comparison with Nijmegen results for np and $pp(c)$ [8,9]. Note that our curve describes properly the average Nijmegen potential results [9] within the corresponding standard deviations. This complies with the fact that we use primarily the np channel to deduce our OBE parameters from a fit but is also an indication of the correctness of the short-distance connection from which our $pp(c)$ phase is predicted. On the other hand, the PWA [8], while compatible with the Nijmegen potentials, is about 2σ away from zero. Certainly, a more sophisticated analysis would be required to reach conclusions at this level of accuracy.

In any case, all implicit effects are contained in the corresponding scattering lengths $\alpha_{0,nn}$ and $\alpha_{0,pp}$. This is actually the remarkable feature about our renormalization construction. In case of having the same potential and kinetic energies, of course scattering lengths coincide. Again, we do not discriminate the short-distance origin of CIB or CSB but rather relate different channels through the kinetic and potential breaking at long distances. As we can see, the short-distance connection can be used to predict the $^1S_0$ phase shifts for the rest of the channels with a high degree of accuracy.

At this point it is worth noting that the ambiguities raised by Sauer [34] for $pp(s)$ are largely limited by the short-distance connection, since by construction short distances in $pp(s)$ and $pp(c)$ are not independent. This is the reason why the short-distance connection works.

V. CONCLUSIONS

In this paper we have analyzed the charge dependence and charge symmetry breaking of the NN interaction. We have used the OBE model with exchange of π, σ, ω, and ρ mesons and we have implemented CIB and CSB by means of pion mass splitting in the OPE potential with different nucleon masses. In particular, and as in previous works [22,23], we have selected the $^1S_0$ np channel to fit scalar meson parameters, m_σ and $g_{\sigma NN}$, as well as vector meson couplings, $g_{\omega NN}$ and $f_{\rho NN}$, to the Nijmegen phase shifts [9]. A fine-tuning problem arises when we use the customary regular boundary condition at the origin $u(0) = 0$. This problem appears in all np, nn, pp, and $pp(c)$ channels and large ($\sim$40%) violations of SU(3) values of the $g_{\omega NN}$ coupling constant are needed. Traditionally, a

[8] Actually, this requires taking into account the strong correlation between $g_{\sigma NN}$ and m_σ found in Ref. [22] since otherwise errors are largely overestimated. Of course, this does not account for the intrinsic error in the short-distance connection itself.

[9] Again, the consideration of statistical $g_{\sigma NN}$-m_σ correlations in the fit proves crucial; if correlations are ignored the errors become about five times larger.

great number of effects such as multimeson exchanges have been essential for explaining the differences in phase shifts and threshold parameters for all np, nn, pp, and $pp(c)$ channels [11–13] or the role played by ρ-ω [38–40] and/or π-η [17] mixing were invoked. These standard approaches need very precise information on the interaction at all distances.

However, once we admit incomplete knowledge of the interaction at short distances, it is possible to sidestep the problem of fine tuning by imposing a renormalization condition; at any stage of the calculation the scattering length is always kept fixed. This renormalization approach embodies short-distance insensitivity. As a consequence, in the charge-independent case, one can comfortably take the experimental and/or SU(3) values for vector meson couplings. For the same reason we can only hope to quantitatively describe the relative changes due to the charge symmetry breaking of the interaction at long distances. These considerations alone allow us to extract some universal information on the symmetry breaking pattern where the np, nn, and pp channels look very much the same at all energies even though the potentials are different and are indeed CIB and CSB. We have used a short-distance condition to relate the renormalized np channel with the others [nn, pp, and $pp(c)$]. This short-distance connection is so far an assumption based on finiteness but we have seen that reasonable results are obtained for low-energy parameters and phase shifts. Our predictions for $(\Delta\alpha_{\rm CIB},\ \Delta r_{\rm CIB})$ and $(\Delta\alpha_{\rm CSB},\ \Delta r_{\rm CSB})$ are compatible with the empirical one within the error estimation. This is in fact a remarkable result: all channels are generated with *just one* scattering length, say np, with the long-distance components of the potential where the CIB and CSB is, via physical pion and nucleon masses, explicitly built in. By taking into account the oversimplified NN OBE force used here, it would be interesting to analyze how our conclusions change with a more realistic NN force.

ACKNOWLEDGMENTS

We thank J. Haidenbauer for a critical reading of the manuscript and L. L. Salcedo for providing his FORTRAN code on Coulomb wave functions. This work has been supported by the Spanish DGI and FEDER funds with Grant No. FIS2008-01143/FIS, Junta de Andalucía Grant No. FQM225-05, Spanish Ingenio-Consolider 2010 Program CPAN (CSD2007-00042) and by the EU Research Infrastructure Integrating Initiative HadronPhysics2 and is authored by a Jefferson Science Associate, LLC, under U.S. Department of Energy Contract No. DE-AC05-06OR23177.

APPENDIX A: SUPERPOSITION PRINCIPLE AND UNIVERSALITY FUNCTIONS

For obtaining the Coulomb extension of Eq. (15) we use the superposition principle to write u_k^C in the following way:

$$C(\eta)\,u_k^C(r) = \left(k\,\cot\delta_0^C\,C^2(\eta) + \frac{2}{a_B}\,h(\eta)\right)u_{k,\rm reg}^C(r) - u_{k,\rm irr}^C(r), \tag{A1}$$

where $u_{k,\rm reg}^C$ and $u_{k,\rm irr}^C$ are solutions of Eq. (16), which obey the asymptotic boundary conditions

$$u_{k,\rm reg}^C(r) \to \frac{F_0(\eta,\rho)}{kC(\eta)}, \tag{A2}$$

$$u_{k,\rm irr}^C(r) \to -C(\eta)\,G_0(\eta,\rho) + \frac{2\eta h(\eta)}{C(\eta)}\,F_0(\eta,\rho), \tag{A3}$$

for $r\to\infty$. These two solutions have been normalized in such a way that the they become analytical around the limit $k\to 0$. With these definitions and using orthogonality to the zero-energy state we obtain

$$\begin{aligned}
\mathcal{A}^C(k) &= u_{0,\rm irr}^C(r_c)u_{k,\rm irr}^{C\,\prime}(r_c) - u_{0,\rm irr}^{C\,\prime}(r_c)u_{k,\rm irr}^C(r_c),\\
\mathcal{B}^C(k) &= u_{0,\rm reg}^{C\,\prime}(r_c)u_{k,\rm irr}^C(r_c) - u_{k,\rm irr}^{C\,\prime}(r_c)u_{0,\rm reg}^C(r_c),\\
\mathcal{C}^C(k) &= u_{0,\rm irr}^C(r_c)u_{k,\rm reg}^{C\,\prime}(r_c) - u_{0,\rm irr}^{C\,\prime}(r_c)u_{k,\rm reg}^C(r_c),\\
\mathcal{D}^C(k) &= u_{0,\rm reg}^{C\,\prime}(r_c)u_{k,\rm reg}^C(r_c) - u_{0,\rm reg}^C(r_c)u_{k,\rm reg}^{C\,\prime}(r_c),
\end{aligned} \tag{A4}$$

where the limit $r_c\to 0$ is understood. Finally, Eq. (24) can be obtained from a low-energy limit of Eq. (15) (see also [35]).

APPENDIX B: PROTON-PROTON FUSION

In this Appendix, we analyze further the consequences of the short-distance connection assumed by Eq. (61). An interesting process is the proton-proton fusion reaction $pp\to d\,e^+\nu_e$, which is of central importance to stellar physics and neutrino astrophysics. The temperature in the Sun core is around $T_c = 15\times 10^6$ K, which means that we have protons of momentum $p\sim(2m_pT_c)^{1/2}\sim 1.1$ MeV. At these low energies, the reaction is dominated by the ${}^1S_0\to d$ nuclear transition. The Gamow-Teller (GT) matrix element [without Meson-Exchange-Currents (MECs)] reads

$$A_S M_{GT} = \int_0^\infty dr\ u_\gamma(r)u_{0,pp}(r), \tag{B1}$$

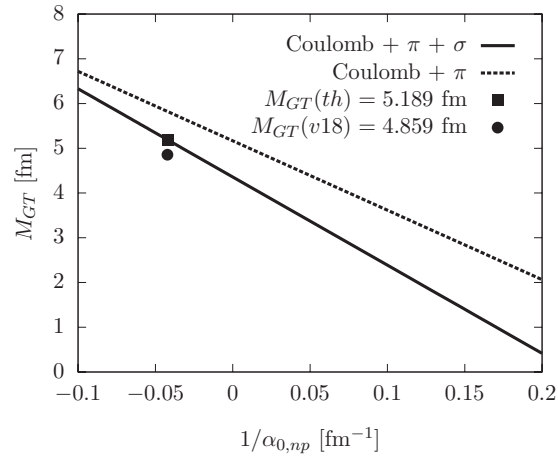

FIG. 7. Dependence of the pp fusion Gamow-Teller matrix element (in femtometers) depending on the singlet np inverse scattering length $1/\alpha_0$ (in fm^{-1}) using the short-distance connection, Eq. (61).

where $u_{0,pp}$ is the zero-energy reduced wave function for the $pp(c)$ system, which can be related to the np problem by Eq. (61). Then taking $\alpha_{0,np}$ as input and integrating inward we can calculate $u_{0,pp}$. For the deuteron we take as a first approximation the normalized bound state, $u_\gamma(r) \to A_S e^{-\gamma_d r}$ with $\gamma_d = 0.2316$ fm^{-1} and integrate inward the Schrödinger equation with negative energy $E = -\gamma_d^2/M_{np}$. We obtain a value $M_{GT} = 5.189$ fm to be compared to a more sophisticated one [37] using Argonne $V18$ wave functions, $M_{GT}|_{AV18} = 4.859$ fm.

In Fig. 7 we show the GT matrix element correlation with the np scattering length compared with the AV18 calculation. Of course, we have not included the tensor force which mixed S and D waves in the calculation of the deuteron. However, we can appreciate that our numbers are not very far from those obtained from much more elaborate calculations [37].

[1] D. H. Wilkinson, *Isospin in Nuclear Physics* (Wiley, New York, 1969).
[2] G. A. Miller, B. M. K. Nefkens, and I. Slaus, Phys. Rep. **194**, 1 (1990).
[3] G. A. Miller, A. K. Opper, and E. J. Stephenson, Annu. Rev. Nucl. Part. Sci. **56**, 253 (2006).
[4] R. Machleidt and I. Slaus, J. Phys. G **27**, R69 (2001).
[5] R. Machleidt, K. Holinde, and C. Elster, Phys. Rep. **149**, 1 (1987).
[6] R. Machleidt, Adv. Nucl. Phys. **19**, 189 (1989).
[7] C. Y. Cheung and R. Machleidt, Phys. Rev. C **34**, 1181 (1986).
[8] V. G. J. Stoks, R. A. M. Klomp, M. C. M. Rentmeester, and J. J. de Swart, Phys. Rev. C **48** 792 (1993).
[9] V. G. J. Stoks, R. A. M. Klomp, C. P. F. Terheggen, and J. J. de Swart, Phys. Rev. C **49**, 2950 (1994).
[10] R. B. Wiringa, V. G. J. Stoks, and R. Schiavilla, Phys. Rev. C **51**, 38 (1995).
[11] G.-Q. Li and R. Machleidt, Phys. Rev. C **58**, 1393 (1998).
[12] G.-Q. Li and R. Machleidt, Phys. Rev. C **58**, 3153 (1998).
[13] R. Machleidt, Phys. Rev. C **63**, 024001 (2001).
[14] R. Machleidt and H. Muther, Phys. Rev. C **63**, 034005 (2001).
[15] S. Biswas, P. Roy, and A. K. Dutt-Mazumder, Phys. Rev. C **78**, 045207 (2008).
[16] J. Hamilton and G. C. Oades, Nucl. Phys. A **424**, 447 (1984).
[17] J. Piekarewicz, Phys. Rev. C **48**, 1555 (1993).
[18] C. R. Howell, arXiv:0805.1177.
[19] A. Gardestig, J. Phys. G **36**, 053001 (2009).
[20] A. C. Fonseca, R. Machleidt, and G. A. Miller, Phys. Rev. C **80**, 027001 (2009).
[21] J. Kirscher and D. R. Phillips, Phys. Rev. C **84**, 054004 (2011).
[22] A. Calle Cordon and E. Ruiz Arriola, Phys. Rev. C **81**, 044002 (2010).
[23] A. Calle Cordon and E. Ruiz Arriola, AIP Conf. Proc. **1030**, 334 (2008).
[24] X. Kong and F. Ravndal, Phys. Lett. B **450**, 320 (1999).
[25] X. Kong and F. Ravndal, Nucl. Phys. A **665**, 137 (2000).
[26] J. Gegelia, Eur. Phys. J. A **19**, 355 (2004).
[27] M. Walzl, U. G. Meissner, and E. Epelbaum, Nucl. Phys. A **693**, 663 (2001).
[28] E. Epelbaum and U.-G. Meissner, Phys. Rev. C **72**, 044001 (2005).
[29] S.-I. Ando, J. W. Shin, C. H. Hyun, and S. W. Hong, Phys. Rev. C **76**, 064001 (2007).
[30] H. A. Bethe, Phys. Rev. **76**, 38 (1949).
[31] J. J. de Swart, M. C. M. Rentmeester, and R. G. E. Timmermans, PiN Newslett. **13**, 96 (1997).
[32] G. P. Lepage, in *Nuclear Physics: Proceedings of the VIII Jorge André Swieca Summer School, Brazil*, edited by C. Do Jordao *et al*. (World Scientific, Singapore, 1997).
[33] D. R. Entem, E. Ruiz Arriola, M. Pavon Valderrama, and R. Machleidt, Phys. Rev. C **77**, 044006 (2008).
[34] P. U. Sauer, Phys. Rev. Lett. **32** 626 (1974).
[35] M. Pavon Valderrama and E. Ruiz Arriola, Phys. Rev. C **80**, 024001 (2009).
[36] M. Abramowitz and I. A. Stegun, *Handbook of Mathematical Functions with Formulas, Graphs, and Mathematical Tables* (Dover, New York, 1964).
[37] T.-S. Park, K. Kubodera, D.-P. Min, and M. Rho, Astrophys. J. **507**, 443 (1998).
[38] P. C. McNamee, M. D. Scadron, and S. A. Coon, Nucl. Phys. A **249**, 483 (1975).
[39] S. A. Coon, M. D. Scadron, and P. C. Mcnamee, Nucl. Phys. A **287**, 381 (1977).
[40] J. L. Friar and B. F. Gibson, Phys. Rev. C **17**, 1752 (1978).